atmosphere

MDPI

Article

Characteristics and Potential Inhalation Exposure Risks of Environmentally Persistent Free Radicals in Atmospheric Particulate Matter and Solid Fuel Combustion Particles in High Lung Cancer Incidence Area, China

Kai Xiao [1], Yichun Lin [1], Qingyue Wang [1,*], Senlin Lu [2,*], Weiqian Wang [1], Tanzin Chowdhury [1], Christian Ebere Enyoh [1] and Mominul Haque Rabin [1]

[1] Graduate School of Science and Engineering, Saitama University, 255 Shimo-Okubo, Sakura-ku, Saitama 338-8570, Japan; xiao.k.662@ms.saitama-u.ac.jp (K.X.); lin.y.852@ms.saitama-u.ac.jp (Y.L.); weiqian@mail.saitama-u.ac.jp (W.W.); risha.chowdhury.bau@gmail.com (T.C.); cenyoh@gmail.com (C.E.E.); rabin.m.h.518@ms.saitama-u.ac.jp (M.H.R.)

[2] School of Environmental and Chemical Engineering, Shanghai University, 99 Shangdalu, Baoshan District, Shanghai 200444, China

* Correspondence: seiyo@mail.saitama-u.ac.jp (Q.W.); senlinlv@staff.shu.edu.cn (S.L.)

Citation: Xiao, K.; Lin, Y.; Wang, Q.; Lu, S.; Wang, W.; Chowdhury, T.; Enyoh, C.E.; Rabin, M.H. Characteristics and Potential Inhalation Exposure Risks of Environmentally Persistent Free Radicals in Atmospheric Particulate Matter and Solid Fuel Combustion Particles in High Lung Cancer Incidence Area, China. *Atmosphere* **2021**, *12*, 1467. https://doi.org/10.3390/atmos12111467

Academic Editor: Courtney Roper

Received: 11 October 2021
Accepted: 4 November 2021
Published: 5 November 2021

Abstract: Environmentally persistent free radicals (EPFRs) were previously considered an unrecognized composition of air pollutants and might help explain the long-standing medical mystery of why non-smokers develop tobacco-related diseases such as lung cancer. However, there is no investigated on EPFRs in Xuanwei rural areas, especially in high prevalence of lung cancer areas. In this study, we selected six types of coal and three types of biomass in Xuanwei, then conducted simulated combustion, and six group of atmospheric particulate matters (APMs) to explore the content and particle size distribution pattern of EPFRs and a new health risk assessment method to evaluate the risk of EPFRs in PM for adults and children. Our results show that the contribution of EPFRs for biomass combustion, coal combustion and APMs were mainly distributed in the size range of <1.1 µm, which accounted for 76.15 ± 4.14%, 74.85 ± 10.76%, and 75.23 ± 8.18% of PM3.3. The mean g factors and ΔHp-p indicated that the EPFRs were mainly oxygen-centered radicals in PM in Xuanwei. The results suggest that the health risk of EPFRs is significantly increased when the particle size distribution of EPFRs is taken into account, and coal combustion particulate matter (174.70 ± 37.86 cigarettes for an adult, 66.39 ± 14.39 cigarettes per person per year for a child) is more hazardous to humans than biomass combustion particulate matter (69.41 ± 4.83 cigarettes for an adult, 26.37 ± 1.84 cigarettes per person per year for), followed by APMs (102.88 ± 39.99 cigarettes for an adult, 39.10 ±15.20 cigarettes per person per year for) in $PM_{3.3}$. Our results provides a new perspective and evidence for revealing the reason for the high incidence of lung cancer in Xuanwei, China.

Keywords: environmentally persistent free radicals; lung cancer; health risk assessment; g factors; Xuanwei

1. Introduction

Lung cancer remains the most prevalent cancer (11.6% of all cases) and the leading cause of cancer deaths worldwide (18.4% of all cancer deaths) [1]. Smoking is the largest preventable cause of lung cancer and contributes to more than 80% of cases of this disease on a global scale [2]. However, women have the highest incidence of lung cancer among non-smokers in Xuanwei, China [3]. The mortality of lung cancer in Xuanwei's rural areas are 27.7/100,000 for men and 25.3/100,000 for women, almost five times that of China's national average (4.97/100,000 for both sexes) [4], it ranks among the top in the world for female lung cancer mortality [5]. However, the etiology of lung cancer in the region

remains unclear and known or suspected risk factors such as tobacco [6], potentially toxic metals [7–9], PAHs [10], and SiO_2 [11,12] may account for only a small fraction of lung cancer cases, necessitating further study.

Induced oxidative stress in the lung has been considered to be one of the most common toxic mechanisms of exposure of humans to atmospheric particulate matters (APMs) [13,14]. Reactive species present within atmospheric particulate matters (APMs) constitute one of the more important aerosol-based factors that affect human health [15–17]. Among different size particles, it has also been established that fine particles, are potentially the most dangerous due to their small size, large surface area, deep penetration and ability to be retained in the lung, and high content of redox cycling organic chemicals [18].

Environmentally persistent free radicals (EPFRs) are a novel class of emerging contaminants, which are similar to carcinogenic tar paramagnetic species in cigarettes that can damage normal cells in the body, induce DNA mutations, accelerate the rate of ageing and increase the risk of disease [19]. Several studies have shown that the concentration of EPFRs in the atmosphere were spatially and temporally inhomogeneous, which is mainly caused by different contributions of emission sources, such as residential fuel, vehicles, and industrial activities [20,21]. They are more environmentally persistent than short-lived radicals and can persist in the medium for long periods of time without even disappearing [22]. The most possible mechanisms of EPFRs are formed at transition metal centers that can be easily reduced when an organic compound chemisorbs. Subsequently, an elimination of water or hydrogen chloride results in chemisorption of the organic molecular adsorbate, and then a single electron transfer from the organic molecule to the transition metal center, which leads to the simultaneous reduction in metal and the formation of EPFRs [23]. Scientists have recently begun to assume that environmentally persistent free radicals within PM, which are a class of strongly oxidizing substances, are possible factors that may be responsible for human acute or chronic pneumonia and lung cancer [16,24]. The toxicity of EPFRs stems from their persistence in the environment coupled with their ability to generate OH, which may lead to the downstream generation of other reactive oxygen species (ROSs) [25] including peroxyl (RO_2) and alkoxyl (RO) radicals. APM-bound EPFRs may directly result in oxidative stress in the lung when exposed to APMs [26]. One possible mechanism for this type of health damage is the continuous conversion of O_2 molecules into reactive oxygen species (ROS) by EPFRs [27].

After an extensive literature survey, we found that the risks posed by PM have been extensively researched [28,29], but the risk attribution of specific components of APMs is far from being fully understood. Observations of EPFRs in PM may provide the key to understanding the carcinogenic behaviour of these particles [27,30,31]. To our knowledge, coal burning, biomass burning, and APMs are considered an important sources of EPFRs [32,33]; furthermore, there is few information available for personal exposure levels of inhaled EPFRs in the high lung cancer incidence areas of Xuanwei, China. Therefore, there is a need to assess exposure to EPFRs. In this study, we selected six types of coal and three types of biomass in Xuanwei, then conducted simulated combustion experiments, and six group of APMs using an Andersen high volume air sampler (Shibata Science Co., Ltd., Saitama, Japan) to explore the content and particle size distribution pattern of EPFRs and health risk assessment of EPFRs in particulate matter produced by different sources, providing new perspectives and evidence to reveal the high incidence of lung cancer in Xuanwei.

2. Materials and Methods

Xuanwei country located in Yunnan Province, southwest China, has the highest incidence and mortality rate of lung cancer [34]. After field investigation and data search, we found that wild pine and poplar trees are widely distributed, and 1.78 million hectares of corn was planted in Yunnan, accounting for 25.61% of the crop area in 2019 (http://stats.yn.gov.cn/; accessed on 22 September 2021). In 2019, about 0.67 billion tons of coal were consumed, which contributed about 23.39% of the national primary energy source and

34.57% of total energy consumption in Yunnan Province, China (http://stats.yn.gov.cn/; accessed on 22 September 2021).

2.1. Sample Collection

Three types of raw biomass (Pine, Corncob, Poplar) from Zhongan Town, and six types of residential raw coal from Bole Town (Luomu coal (LM) and Bole coal (BL)), Houshou Town (Lijiawu coal (LJW)), Laochang Town (Shunfa coal (SF)), Laibin Town (Guangming coal (GM) and Zongfan coal (ZF)), and six groups of APMs (Houshou Town) were collected. The sampling sites were shown in the Supplementary Materials Figure S1.

Then, simulated combustion on raw coal and biomass was conducted via a burning system, which was simulated according to local residents' combustion mode in our laboratory (in the Supplementary Materials Figure S2). In addition to the above, six sample groups of APMs (A–H) were conducted by a high-volume air sampler (Shibata Science Co., Ltd., Saitama, Japan) at a flow rate of 566 L/min in Xuanwei local rural residences in February and March in 2017 (Table S1), and the aerodynamic diameters were <1.1 μm, 1.1–2.0 μm, 2.0–3.3 μm, 3.3–7.0 μm, and >7.0 μm. The detailed information of raw coal, biomass, and APMs is shown in Table 1. More information on the burning system and pre-treatment and post-treatment of samples can be found in our previous study [28].

Table 1. The detail information of raw coal, biomass and APMs from Xuanwei.

Types	Mine	Sample Groups	Location	Altitude/m	Latitude	Longitude
Coal	Luomu	LM	Bole Town	1793	26°29′34.09″	103°46′9.17″
	Bole	BL	Bole Town	2104	25°47′15.32″	104°07′32.32″
	Zongfan	ZF	Laibin Town	2024	26°17′58.25″	104°05′42.49″
	Guangming	GM	Laibin Town	1987	26°19′46.55″	104°09′36.43″
	Shunfa	SF	Laochang Town	1994	25°13′31.13″	104°31′22.42″
	Lijiawu	LJW	Housuo Town	2078	25°79′99.21″	104°28′60.06″
Biomass		Corncob	Zhongan Town	1831	25°39′58.85″	104°15′8.20″
		Pine	Zhongan Town	1831	25°39′58.85″	104°15′8.20″
		Poplar	Zhongan Town	1812	25°40′38.06″	104°15′9.59″
APMs		A~D	Housuo Town	2023	25°50′59″	104°23′22″
		E~F	Housuo Town	2267	25°49′37″	104°14′15″

2.2. Detection of EPFRs

Electron spin resonance (ESR) spectroscopy was used to determine EPFRs. To determine EPFRs, quartz fiber filters were cut into strips of 3–4 mm, then added to a quartz EPR tube and measured on the corresponding instrument. The relevant parameters were as follows: sweep time, 120 s; center field 324.74 mT; sweep width, 25 mT; modulation frequency, 100 kHz; modulation Width, 0.05 mT; microwave frequency 9105.26 MHz; and microwave power, 0.998 mW.

2.3. Data Processing and Calculation of the Absolute Number of Spins

ESR tests were performed on standards containing Mn (II) to calibrate the absolute number of spins and then characteristic parameters such as the g factor, and ΔHp-p of the EPFRs were obtained. The formula used to calculate the spin numbers and g factors are shown in Equations (1) and (2) [35–37]:

$$g = 0.07145 \times ƛ\ (\text{MHz})/H\ (\text{mT}) \quad (1)$$

$$\text{Spins}_{\text{sample}}\ (\text{spins/g}) = 3.02 \times 10^{14}\ (\text{spins/g}) \times \text{Integral}_{\text{sample}}/\text{Integral}_{\text{standard}} \quad (2)$$

where g is the electron spin g-factor of the particle, ƛ (MHz) represents the microwave frequency, H (mT) is the resonance magnetic field strength during the measurements;

3.02×10^{14} is the total spins of the standard Mn, $Spins_{sample}$ is the spin concentration of the unknown sample, $Integral_{sample}$ and $Integral_{standard}$ represent the signal integration areas of the sample and Mn (II) standard, respectively [37]. The sample atmospheric spin concentrations of EPFRs (spins/m^3) were calculated as the total spin divided by the total sample volume. The EPFR spin concentrations in PM masses (spins/g) were determined as the total spin divided by the collected PM mass.

2.4. EPFRs Exposure Evaluation

To date, there is no internationally accepted method to assess the health risk of EPFRs in PM. Several methods are used to assess the health risks of EPFRs [33,38–40]; however, all of them evaluate EPFRs inhalation risk for adults, not children. In our study, we use the equivalent number of cigarettes to evaluate the potential health risks of EPFRs in PM for Xunawei residents [31].The exposure level is provided in Equations (3) and (4):

$$Inh_{PM} = RC_{PM} \times F \times Fr \times PC_{PM} \times Rinhalation \quad (3)$$

$$N_{cig} = 30 \times Inh_{PM}/RC_{cig} \times C_{tar} \quad (4)$$

where Inh_{PM} is the daily EPFRs exposure from inhaled PM (spins/g/day); F is the conversion from g to micrograms (1×10^{-6}) [31], Fr is the alveolar fraction retained in the lung (0.75). PC_{PM} is the concentration of PM (μg/m^3) and R inhalation represents the daily amount of air inhaled (20 m^3/day for an adult [41], 7.6 m^3/day for a child) (https://www.epa.gov/risk/risk-assessment-guidance-superfund-rags-part; accessed on 24 September 2021). N_{cig} represents the number of cigarettes (person/year), 30 represents 30 days per month. RCcig (4.75×10^{16} spins/g) [38] indicates the concentration of free radicals in cigarette tar, and Ctar (0.013 g/cig) indicates the amount of tar per cigarette [31].

3. Results and Discussion

The size of particulate matter is directly related to their potential to cause health problems. Fine particles ($PM_{2.5}$) pose the greatest health risk. These fine particles can penetrate deep into the lungs and some may even enter the bloodstream, and can affect a person's lungs and heart. Coarse particles ($PM_{2.5–10}$) are of less concern, although they can irritate a person's eyes, nose, and throat. Therefore, in this study we focus on particle sizes <1.1 μm, 1.1–2.0 μm and 2.0–3.3 μm. Numerous studies have been conducted on EPFRs in atmospheric particulate matter [22,26,32,42], but there is a lack of studies on EPFRs in particulate matter emitted directly from raw coal combustion and biomass combustion.

3.1. EPFRs and PM Concentrations in Atmospheric Particulate Matter and Solid Fuel Combustion Particles

3.1.1. EPFRs and PM Concentrations in Biomass Combustion Particles

The concentration distributions of EPFRs and PM in simulated particulate matter emitted from biomass combustion (corncobs, pine, poplar) were provided in Figure 1 and Table S2. The concentrations of EPFEs and PM emitted from the three-biomass combustion were significantly different in the particle size ranges <1.1, 1.1–2.0 and 2.0–3.3 μm. Both the EPFRs and the PM concentration reach their maximum at <1.1 μm, while the lowest concentration is found at the particle size 2.0–3.3 μm. The atmospheric concentrations of EPFRs percentage mean value of $PM_{1.1}$, $PM_{1.1–2.0}$, and $PM_{2.0–3.3}$ were 76.25 ± 4.14%, 13.69 ± 3.95%, and 10.06 ± 0.23%, which corresponded to PM mass concentrations were 2948.77 ± 1438.66 μg/m^3, 1415.44 ± 712.85 μg/m^3 and 1087.57 ± 504.44 μg/m^3, respectively (Table 2). The atmospheric concentrations of EPFRs in the $PM_{1.1}$ were 4.51×10^{17}, 4.27×10^{17} and 3.26×10^{17} spins/m^3 for corncob, pine, and poplar, respectively, while the mean atmospheric concentrations in $PM_{1.1}$ were found to be several times $PM_{1.1–2.0}$ (6.34 ± 2.67) and $PM_{2.0–3.3}$ (7.60 ± 0.57). The EPFR concentrations in the $PM_{1.1}$ at the three sites were 3.11×10^{15}, 3.37×10^{15} and 1.08×10^{15} spins/g for corncob, pine and poplar, respectively (shown in Table S2). It has been reported that the EPFR concentrations in $PM_{2.5}$

from the corn straw, rice straw, jujube wood, and pine wood (four biomass, purchased from Jiangsu province) were in the range of 0.9×10^{19} spins/g to 6.1×10^{19} spins/g [33], the average radical intensities in PM emissions from fatwood and pine wood were 1.2×10^{18}, and 9.1×10^{17} spins/gram, respectively [43]. Compared with previous studies, the EPFR concentrations in $PM_{3.3}$ (the range of 1.99×10^{15} spins/g to 5.50×10^{15} spins/g) were 2–4 orders of magnitude lower than those reported in a previous study. EPFRs were mainly concentrated in the size range of <1.1 µm, which accounted for 76.25 ± 4.15% of $PM_{3.3}$, indicating that the $PM_{1.1}$ emitted biomass combustion is more harmful to the human body than $PM_{2.0–3.3}$ and $PM_{2.0–3.3}$; therefore, deserves more in-depth study.

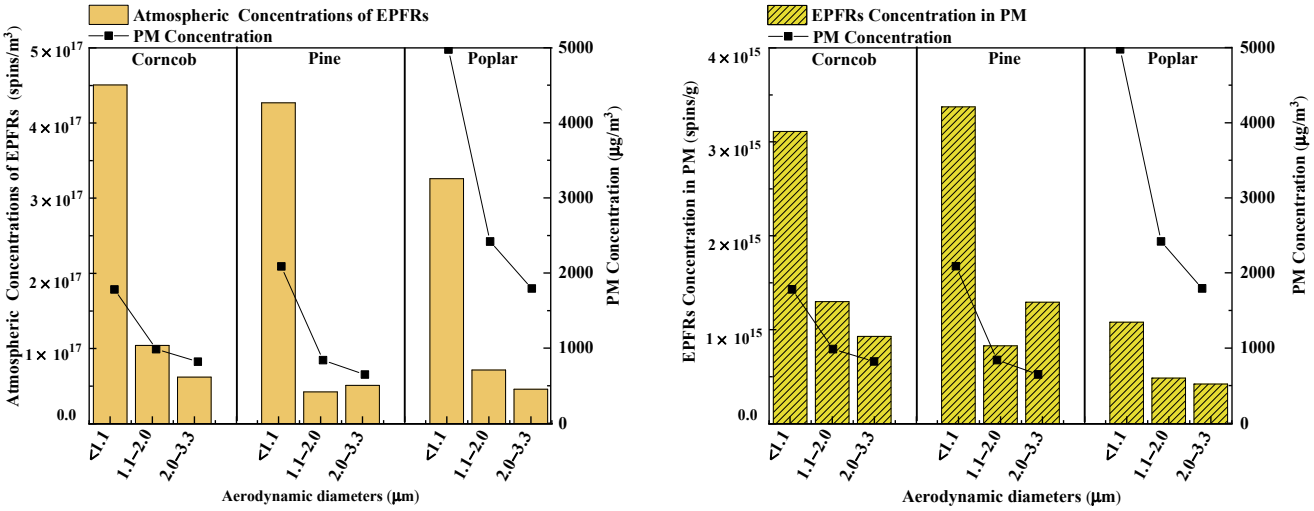

Figure 1. EPFRs and PM concentrations in biomass combustion particles from Xuanwei (the **left**: the atmospheric EPFRs concentrations; the **right**: EPFRs concentrations in PM).

Table 2. Size distribution of EPFRs and PM in simulated biomass combustion particles from Xuanwei (%).

Sample Groups	$PM_{1.1}/PM_{3.3}$ (%)			$PM_{1.1–2.0}/PM_{3.3}$ (%)			$PM_{2.0–3.3}/PM_{3.3}$ (%)		
	Spins/m^3	Spins/g	µg/m^3	Spins/m^3	Spins/g	µg/m^3	Spins/m^3	Spins/g	µg/m^3
Corncob	73.11	58.26	49.66	16.86	24.35	27.48	10.03	17.38	22.86
Pine	82.10	61.40	58.39	8.11	15.10	23.49	9.79	23.50	18.13
Poplar	73.56	54.33	54.14	16.09	24.45	26.33	10.36	21.23	19.52
Average	76.25	57.99	54.06	13.69	21.30	25.77	10.06	20.70	20.17
Min	73.11	54.33	49.66	8.11	15.10	23.49	9.79	17.38	18.13
Max	82.10	61.40	58.39	16.86	24.45	27.48	10.36	23.50	22.86
STD	4.14	2.89	3.56	3.95	4.38	1.68	0.23	2.52	1.99

3.1.2. EPFRs and PM Concentrations in Coal Combustion Particles

Table 3 lists the size distribution of EPFRs and PM in simulated coal combustion particles (%). Figure 2 and Table S3 shows the EPFRs and PM concentrations in coal combustion particles. The atmospheric EPFRs concentrations in $PM_{1.1}$, $PM_{2.0–3.3}$ and $PM_{2.0–3.3}$ make the contribution to $PM_{3.3}$ 74.85 ± 10.76%, 13.10 ± 7.66%, and 12.05 ± 7.25%, respectively. The average atmospheric concentrations in $PM_{1.1}$ were found to be several times the $PM_{1.1–2.0}$ (8.81 ± 6.70) and $PM_{2.0–3.3}$ (8.07 ± 3.68). The concentration distribution of EPFRs and PM in coal combustion emission particulate matter is similar to that of biomass combustion particulate matter, both mainly concentrated in the <1.1 um particle size. The mean atmospheric concentrations of EPFRs in the $PM_{1.1}$, $PM_{2.0–3.3}$ and $PM_{2.0–3.3}$ were $2.16 \times 10^{17} \pm 5.82 \times 10^{16}$ spins/m^3, $3.70 \times 10^{16} \pm 2.32 \times 10^{16}$ spins/m^3 and $3.67 \times 10^{16} \pm 2.89 \times 10^{16}$ spins/m^3, which corresponded to PM mass concentrations 3806.19 ± 2105.99 µg/m^3, 1537.84 ± 565.64 µg/m^3 and 1404.60 ± 672.75 µg/m^3, respec-

tively (shown in Table S3). Compared with previous studies, the EPFR concentrations in $PM_{3.3}$ (the range of 4.13×10^{15} spins/g to 1.78×10^{16} spins/g) which were 1–4 orders of magnitude lower than those reported in a previous study for the total particular matter from bituminous coal (4.4×10^{17} spins/g), anthracite (2.3×10^{17} spins/g) [43], and bituminous (10^{19} spins/g), which were purchased from Henan Province.

Table 3. Size distribution of EPFRs and PM in simulated coal combustion particles from Xuanwei (%).

Sample Groups	$PM_{1.1}/PM_{3.3}$ (%)			$PM_{1.1–2.0}/PM_{3.3}$ (%)			$PM_{2.0–3.3}/PM_{3.3}$ (%)		
	Spins/m^3	Spins/g	μg/m^3	Spins/m^3	Spins/g	μg/m^3	Spins/m^3	Spins/g	μg/m^3
BL	58.15	51.66	40.00	14.00	18.72	26.58	27.85	29.61	33.42
LM	63.74	52.12	46.46	28.09	28.37	37.62	8.17	19.51	15.92
SF	81.77	56.06	56.29	7.07	8.66	31.50	11.16	35.27	12.21
LJW	89.86	81.85	43.81	4.03	4.14	38.77	6.12	14.01	17.43
GM	78.85	71.34	42.23	10.76	12.24	33.60	10.39	16.42	24.17
ZF	76.76	58.53	50.35	14.64	15.16	37.10	8.60	26.31	12.55
Average	74.85	61.93	46.52	13.10	14.55	34.19	12.05	23.52	19.28
Min	58.15	51.66	40.00	4.03	4.14	26.58	6.12	14.01	12.21
Max	89.86	81.85	56.29	28.09	28.37	38.77	27.85	35.27	33.42
STD	10.76	11.05	5.45	7.66	7.71	4.22	7.25	7.53	7.46

STD: Standard Deviation.

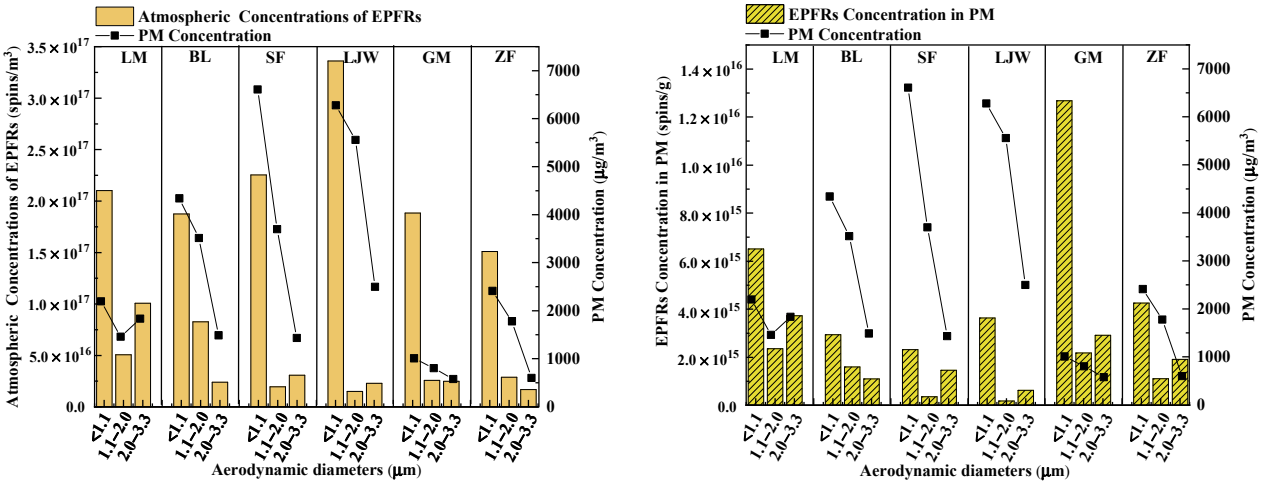

Figure 2. EPFRs and PM concentrations in coal combustion particles from Xuanwei (the **left**: the atmospheric EPFRs concentrations; the **right**: EPFRs concentrations in PM).

3.1.3. EPFRs and PM Concentrations in Atmospheric Particulate Matters

The mass concentrations of three PM fractions classified as $PM_{<1.1}$, $PM_{1.1–2.0}$, and $PM_{2.0–3.3}$, were 42.92 ± 16.50 μg/m^3, 26.33 ± 5.66 μg/m^3, and 20.42 ± 2.68 μg/m^3, respectively (shown in Figure 3 and Table S4). As shown in Table 4, the $PM_{1.1}$ fraction contributed 46.56% ± 9.67% of the $PM_{3.3}$ mass, which indicated that much more PM in the atmosphere was present in smaller size fractions.

The mean atmospheric concentrations of EPFRs in $PM_{1.1}$, $PM_{1.1–2.0}$, and $PM_{2.0–3.3}$ were $7.03 \times 10^{15} \pm 5.29 \times 10^{15}$ spins/m^3, $9.05 \times 10^{14} \pm 2.50 \times 10^{14}$ spins/m^3, and $8.35 \times 10^{15} \pm 3.06 \times 10^{15}$ spins/m^3, respectively, while the mean concentrations in PM were in the range of $2.16 \times 10^{17} \pm 9.73 \times 10^{16}$ spins/g, $5.38 \times 10^{16} \pm 1.72 \times 10^{16}$ spins/m^3, and 8.35×10^{14} ± to 3.06×10^{14} spins/m^3, respectively. Several other studies have reported EPFR concentrations in atmospheric particulate matter, in $PM_{2.5}$ in Taif, Saudi Arabia. Saudi Arabia ranged from 1.6×10^{16} to 5.8×10^{16} spins/m^3 [44], and in $PM_{2.5}$ in Xuanwei, China ranged from 3.20×10^{17} to 3.10×10^{19} spins/g [45]. In $PM_{2.5}$ in Xi'an ranged from 9.8×10^{11} to 6.9×10^{14} spins/m^3 [38]. In $PM_{2.5}$ samples from Baton Rouge,

ranged from 2.46 × 10^{16} to 2.79 × 10^{17} spins/g [31]. The concentrations of EPFRs were lower. The level of EPFR concentration in PM in Xuanwei was several times smaller than that in previous studies. However, in our study, the levels of EPFRs in the PM were dozens of times lower than previous reported EPFR concentrations. EPFRs were mostly present in the $PM_{1.1}$ fraction, in which the EPFR concentration was 3.43–19.85 times higher than that in $PM_{1.1–2.0}$ and 4.09–15.47 times higher than that in $PM_{2.0–3.3}$, which were in agreement with previous research [46]. In addition, it is worth noting that $PM_{2.0}$ can enter the lungs and even the bloodstream more deeply than coarse particles, which may induce harmful reactive oxygen species (ROS) and DNA damage [47].

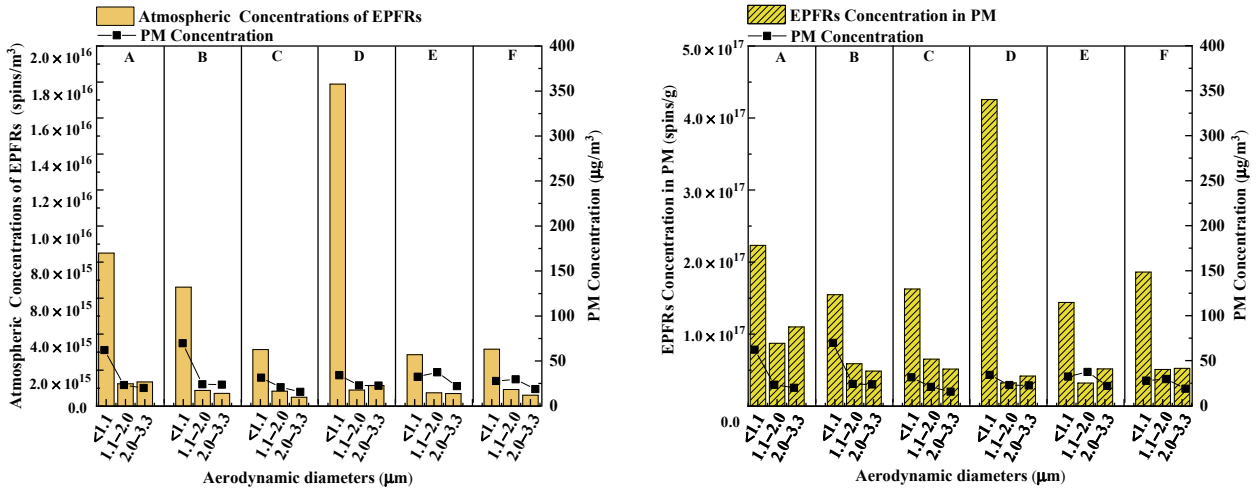

Figure 3. EPFRs and PM concentrations in atmospheric particulate matters from Xuanwei. (The **left**: the atmospheric EPFRs concentrations; the **right**: EPFRs concentrations in PM).

Table 4. Size distribution of EPFRs and PM in atmospheric particulate matters from Xuanwei (%).

Sample Groups	$PM_{1.1}/PM_{3.3}$ (%)			$PM_{1.1–2.0}/PM_{3.3}$ (%)			$PM_{2.0–3.3}/PM_{3.3}$ (%)		
	Spins/m^3	Spins/g	μg/m^3	Spins/m^3	Spins/g	μg/m^3	Spins/m^3	Spins/g	μg/m^3
A	76.71	53.07	58.97	11.19	20.75	22.09	12.09	26.18	18.94
B	80.72	58.98	59.38	10.64	22.45	20.50	8.65	18.57	20.12
C	70.31	58.26	46.29	18.61	23.30	30.66	11.08	18.44	23.05
D	89.67	85.22	42.99	4.51	6.44	28.66	5.81	8.34	28.36
E	66.54	63.16	35.27	17.19	14.08	40.81	16.26	22.76	23.91
F	67.43	64.23	36.45	19.66	17.58	38.87	12.91	18.20	24.67
Average	75.23	63.82	46.56	13.63	17.43	30.26	11.14	18.75	23.18
Min	66.54	53.07	35.27	4.51	6.44	20.50	5.81	8.34	18.94
Max	89.67	85.22	59.38	19.66	23.30	40.81	16.26	26.18	28.36
STD	8.18	10.23	9.67	5.35	5.81	7.64	3.29	5.48	3.08

STD: Standard Deviation.

In our study, the simulated combustion experiments with raw coal and biomass were carried out in a relatively closed room, so the mass concentrations of collected particulate matter were much higher than those collected in open areas. Our results indicate that EPFRs attach more readily to fine particles, which may be due to the fact that fine particles have larger surface areas and more porous surfaces, leading to higher adsorption and retention of EPFRs [17,46,48]. The distribution pattern in Figures 2–4 showed that EPFR concentrations in each PM fraction increased as the particle size decreased. The main reason for the low concentration of EPFRs in our samples may be that our samples have been stored for too long, resulting in partial degradation. The above results suggest that the concentration of EPFRs in atmospheric particulate matter varies across regions and different combustion sources. However, to the best of our knowledge, the current studies on

the concentrations of EPFRs in atmospheric particulate matter are limited to a few regions and a limited number of samples. In addition, more studies on EPFRs concentrations in atmospheric particulate matter samples from different regions, particle sizes, and sources are needed.

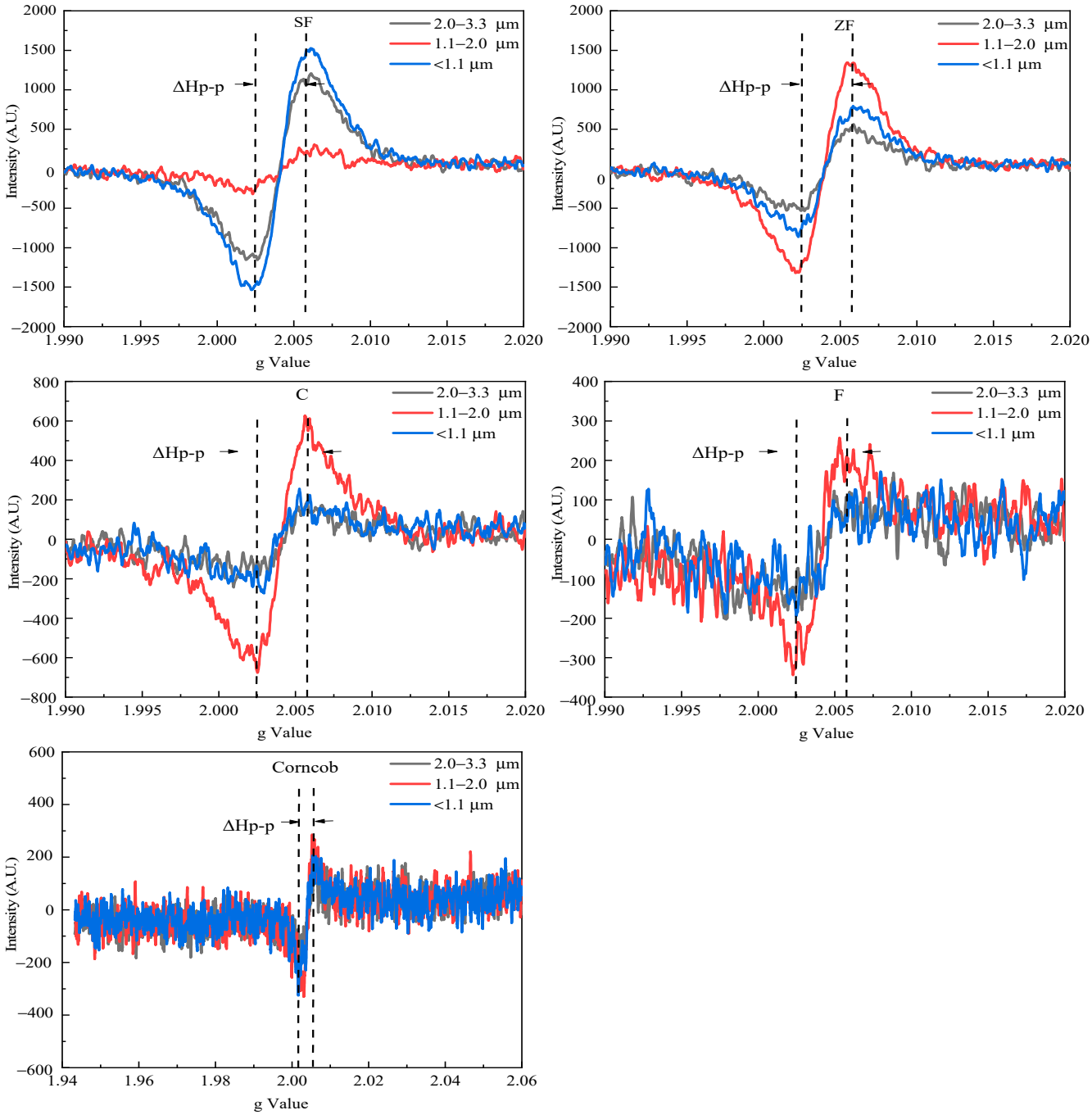

Figure 4. The mean g factor and ΔHp-p of the EPFRs.

3.2. EPFRs Species Characteristics

The g-factor and peak width (referred to as ΔHp-p, Gauss) were important parameters for identifying the type of free radicals [17,44], the average ΔHp-p was calculated to find the distance between the maximum and minimum y-axis values on the x-axis [37]. According to previous reports, carbon-centered radicals are generally less than 2.003, oxygen-centered

radicals are generally greater than 2.0040, and *g* factors in the range of 2.0030–2.0040 are believed to correspond to a mixture of carbon- and oxygen-centered radicals [23,49,50].

A comparison of the EPR spectra of EPFRs in different PMs (as shown in Figure 4) indicates that the g-factors in PMs were different and the signal intensity of EPFRs is also different (The g-value for the other samples can be seen in Figures S3–S5). The mean g factor and ΔHp-p of the EPFRs (Table S5) were ranged from 2.0036 to 2.0040 and 5.8519 to 5.8885 G for PM from coal combustion, ranged from 2.0040 to 2.0041 and 3.7846 to 6.9807 G for PM from biomass combustion, and ranged from 2.0042 to 2.0043 and 5.6444 to 8.7616 G for APMs, indicating that the samples were mainly oxygen-centered radicals (phenoxyl and semiquinone radicals) in Xuanwei. In addition, the small ΔHp-p variability of EPFRs in biomass combustion particulate matter, raw coal combustion particulate matter, and APMs also indicates that EPFRs are of the same type, but contains various organic species or organometallic combinations [27,51].

Research found that coal has a high g-value of 2.0046 in Xuanwei [45], and the g-factors of EPFRs in atmospheric particles vary from 2.0030 to 2.0047 and $\Delta H_{p\text{-}p}$ of 4.7–7.9 G [27], which are typical of oxygen-centered or oxygen-containing EPFRs, for example, phenoxyl and semiquinone radicals [45,46,52]. In general, both oxygen-centered and carbon-centered radicals are present in atmospheric particulate matter, as oxygen-centered radicals tend to adhere to fine particles, while carbon-centered radicals mostly adhere to coarse particles. For fine particles, more of the porous structure is exposed, thus providing more available active and adsorption sites for EPFRs [53].

Moreover, the presence of semiquinone and phenoxy radicals may lead to activated species in the fine particulate matter in the environment [54,55]. Thus, oxygen-centered radicals appear to be more toxic with fine particles because of their direct effects on the human body; carbon-centered radicals on coarse particles should also be emphasized because of their environmental impact [46,53].

4. Potential Health Risk of EPFRs

In our study, the main types of EPFRs in PM were phenoxyl and semiquinone radicals. The spectral characteristics of EPFRs were compared with that of cigarette tar, both of them were similar to semiquinone radicals, and identified as semiquinone radicals [56,57], which associated with a quinone/hydroquinone redox cycle capable of producing reactive oxygen species (ROS), to be involved in the carcinogenicity [40].

In this study, to assess the potential health risk of EPFRs in biomass combustion particulate matter, coal combustion particulate matter and APMs for Xuanwei residents, we used the equivalent of cigarettes to represent the potential health risk of EPFRs for adults and children per person per year (Table S6). Our results showed that the average amount of EPFRs exposure were equivalent to 130.31 ± 35.06 cigarettes for an adult, 49.52 ± 13.32 cigarettes for a child in $PM_{1.1}$, 42.97 ± 43.51 cigarettes for an adult, 16.33 ± 16.54 cigarettes for a child in $PM_{1.1–2.0}$, and 22.09 ± 17.40 cigarettes for an adult, 8.39 ± 6.61 cigarettes for a child in $PM_{2.0–3.3}$ from coal combustion, respectively. The exposure levels in $PM_{1.1}$ were 1.00–22.32 times higher than in $PM_{1.1–2.0}$, and 2.09–14.69 times higher than in $PM_{2.0–3.3}$ for both adult and child, which indicates that EPFRs in $PM_{1.1}$ are the most harmful to humans. Meanwhile, the estimated results of EPFRs emission biomass combustion showed that the average EPFRs exposure was equivalent to 53.11 ± 6.65 cigarettes for an adult, 20.18 ± 2.53 cigarettes for a child in $PM_{1.1}$, 9.33 ± 2.26 cigarettes for an adult, 3.54 ± 0.86 cigarettes for a child in $PM_{1.1–2.0}$, and 6.97 ± 0.34 cigarettes for an adult, 2.65 ± 0.13 cigarettes for a child in $PM_{2.0–3.3}$ per year, respectively. In contrast, the average EPFRs exposure in APMs were equivalent to 80.02 ± 37.37 cigarettes for an adult, 30.41 ± 14.20 cigarettes for a child in $PM_{1.1}$, 31.57 ± 31.27 cigarettes for an adult, 12.00 ± 11.88 cigarettes for a child in $PM_{1.1–2.0}$, and 11.44 ± 4.06 cigarettes for an adult, 4.35 ± 1.54 cigarettes for a child in $PM_{2.0–3.3}$ per day, respectively. Previous studies have shown that EPFRs inhaled from $PM_{2.5}$ can cause human health risks comparable with 0.4–0.9 cigarettes per day [31], 5.0 cigarettes in $PM_{2.5}$ per

person per day in Xi'an in 2017 [38], 46 cigarettes in $PM_{2.5}$ per day in airborne particulate matter in Beijing [19], 2.3–6.8 cigarettes per capita per day in Wanzhou, China [22]. The above results indicate that the potential health risks of EPFRs in PM varies from region to region and from one combustion source to another.

The results of this study suggest that the health risk of EPFRs is significantly increased when the particle size distribution of EPFRs is taken into account, and coal combustion particulate matter is more hazardous to humans than combustion particulate matter, followed by APMs.

5. Conclusions and Limitations of the Study

Coal combustion, biomass burning and APMs are considered to be important sources of EPFRs, and in addition, there is little information on individual exposure levels of inhaled EPFRs in the high lung cancer prevalence area of Xuanwei, China. However, the most important thing is that the mechanism of the high lung incidence is not clear. In this study, we conducted simulated combustion experiments (six types of coal, three types of biomass), and six groups of atmospheric particulate matter were collected to explore the content and particle size distribution pattern of EPFRs and potential health risk of EPFRs for adults and children, providing new perspectives and evidence to reveal the high incidence of lung cancer in Xuanwei.

5.1. Conclusions

(1) The contribution of EPFRs for biomass combustion, coal combustion and APMs were mainly distributed in the size range of <1.1 μm, which accounted for 76.15 ± 4.14%, 74.85 ± 10.76%, and 75.23 ± 8.18% of $PM_{3.3}$, respectively;

(2) The mean g factors were ranged from 2.0016 to 2.0043, 2.0039 to 2.0043 and 2.0039 to 2.0046 for biomass combustion, coal combustion and APMs, respectively, indicating that the samples were mainly oxygen-centered radicals (phenoxyl and semiquinone radicals) in Xuanwei;

(3) The potential health risks of EPFRs for adults and children in $PM_{1.1}$ were equivalent to 130.31 ± 35.06, 49.52 ± 13.32 cigarettes in coal combustion particles, 53.11 ± 6.65, 20.18 ± 2.53 cigarettes in biomass combustion particles, and 80.02 ± 37.37, 30.41 ± 14.20 cigarettes in APMs, respectively.The results suggest that the health risk of EPFRs is significantly increased when the particle size distribution of EPFRs is taken into account, and coal combustion particulate matter is more hazardous to humans than biomass combustion particulate matter, followed by APMs.

5.2. Limitations of the Study

There are significant differences in the concentrations and potential health risks in particles of different sizes, and these differences are due to the influence of the source and generation process. In view of the complexity and diversity of the formation process of EPFRs in the actual atmospheric particulates, and EPFR is a formation mechanism that should be more comprehensively studied in the future. There is a lack of information on the ROS generated by the EPFRs transition metal oxide combination through the cellular matrices and tissue. Some attempts should be performed in cell-free and cell-based experiments to obtain well-characterized information about the ROS generated by the EPFRs transition metal oxide combination and to better address the health effects of EPFRs.

Supplementary Materials: The following are available online at https://www.mdpi.com/article/10.3390/atmos12111467/s1, Figure S1: Sampling sites, Figure S2: Sketch of sampling system, Figure S3: The EPR spectra of EPFRs in APMs particulate matters, Figure S4: The EPR spectra of EPFRs in biomass burning particulate matters, Figure S5: The EPR spectra of EPFRs in coal burning particulate matters, Table S1: Records of atmospheric particulate matter collected in Yunnan residential areas in 2017, Table S2: EPFRs and PM concentrations in biomass combustion particles, Table S3: EPFRs and PM concentrations in coal combustion particles, Table S4: EPFRs and PM concentrations in atmospheric particulate matters, Table S5: g- values and ΔH_{p-p} of the EPFRs produced by different PM from Xuanwei, Table S6; The potential health risk of EPFRs for adults and child per year.

Author Contributions: Conceptualization, K.X. and Q.W.; methodology, S.L., W.W. and Y.L.; software, K.X., validation, W.W. and S.L.; formal analysis, K.X. and Q.W.; investigation, Q.W.; resources contribution, Q.W.; data curation, K.X. and Q.W.; writing—original draft preparation, K.X.; writing—review and editing, K.X., S.L., T.C., C.E.E., M.H.R. and Q.W.; visualization, K.X.; supervision, K.X. and Q.W.; project administration, Q.W.; funding acquisition, Q.W. All authors have read and agreed to the published version of the manuscript.

Funding: This study was partially supported by the Special Funds for Innovative Area Research (No. 20120015, FY2008-FY2012) and Basic Research (B) (No. 24310005, FY2012-FY2014; No.18H03384, FY2017~FY2020) of Grant-in-Aid for Scientific Research of Japanese Ministry of Education, Culture, Sports, Science and Technology (MEXT) and the Steel Foundation for Environmental Protection Technology of Japan (No. C-33, FY 2015-FY 2017).

Acknowledgments: I would like to express my gratitude to Shanghai Institute of Applied Physic, Chinese Academy of Sciences, where I test EPFRs.

Conflicts of Interest: The authors declare that they have no conflict of interest.

Abbreviations

APMs	Atmospheric particulate matters
BL	Bole
Ctar	The amount of tar per cigarette
EPFRs	Environmentally Persistent Free Radicals
ESR	Electron spin resonance
H	Field strength
GM	Guangming coal
LJW	Lijiawu coal
LM	Luomu
ƛ	Microwave frequency
N_{cig}	The number of cigarettes
$Integral_{sample}$	The signal integration areas of the sample
$Integral_{standard}$	The signal integration areas of the sample
PC_{PM}	The concentration of PM
ROS	Reactive oxygen species
RCcig	The concentration of free radicals in cigarette tar
SF	Shunfa coal
$Spins_{sample}$	The spin concentration of the unknown sample
ZF	Zongfan coal

References

1. Bray, F.; Ferlay, J.; Soerjomataram, I.; Siegel, R.L.; Torre, L.A.; Jemal, A. Global cancer statistics 2018: GLGLO BOCAN estimates of incidence and mortality worldwide for 36 cancers in 185 countries. *CA Cancer J. Clin.* **2018**, *68*, 394–424. [CrossRef] [PubMed]
2. Kulhánová, I.; Forman, D.; Vignat, J.; Espina, C.; Brenner, H.; Storm, H.H.; Soerjomataram, I. Tobacco-related cancers in Europe: The scale of the epidemic in 2018. *Eur. J. Cancer* **2020**, *139*, 27–36. [CrossRef] [PubMed]
3. Cao, M.; Chen, W. Epidemiology of lung cancer in China. *Thorac. Cancer* **2019**, *10*, 3–7. [CrossRef]
4. Li, J.; Guo, W.; Ran, J.; Tang, R.; Lin, H.; Chen, X.; Huang, Y. Five-year lung cancer mortality risk analysis and topography in Xuan Wei: A spatiotemporal correlation analysis. *BMC Public Health* **2019**, *19*, 173. [CrossRef] [PubMed]
5. Hosgood, H.D., III; Sapkota, A.R.; Rothman, N.; Rohan, T.; Hu, W.; Xu, J.; Lan, Q. The potential role of lung microbiota in lung cancer attributed to household coal burning exposures. *Environ. Mol. Mutagen.* **2014**, *55*, 643–651. [CrossRef] [PubMed]

6. Sheng, L.; Tu, J.W.; Tian, J.H.; Chen, H.J.; Pan, C.L.; Zhou, R.Z. A meta-analysis of the relationship between environmental tobacco smoke and lung cancer risk of nonsmoker in China. *Medicine* **2018**, *97*, e11389. [CrossRef] [PubMed]
7. Lu, S.; Yi, F.; Hao, X.; Yu, S.; Ren, J.; Wu, M.; Wang, Q. Physicochemical properties and ability to generate free radicals of ambient coarse, fine, and ultrafine particles in the atmosphere of Xuanwei, China, an area of high lung cancer incidence. *Atmos. Environ.* **2014**, *97*, 519–528. [CrossRef]
8. Feng, X.; Shao, L.; Xi, C.; Jones, T.; Zhang, D.; BéruBé, K. Particle-induced oxidative damage by indoor size-segregated particulate matter from coal-burning homes in the Xuanwei lung cancer epidemic area, Yunnan Province, China. *Chemosphere* **2020**, *256*, 127058. [CrossRef] [PubMed]
9. Xiao, K.; Qin, A.; Wang, W.; Lu, S.; Wang, Q. Study on the Characteristics of Size-Segregated Particulate Water-Soluble Inorganic Ions and Potentially Toxic Metals during Wintertime in a High Population Residential Area in Beijing, China. *Processes* **2021**, *9*, 552. [CrossRef]
10. Wang, R.; Huang, Q.; Cai, J.; Wang, J. Seasonal variations of atmospheric polycyclic aromatic hydrocarbons (PAHs) surrounding Chaohu Lake, China: Source, partitioning behavior, and lung cancer risk. *Atmos. Pollut. Res.* **2021**, *12*, 101056. [CrossRef]
11. Tian, L.; Lucas, D.; Fischer, S.L.; Lee, S.C.; Hammond, S.K.; Koshland, C.P. Particle and gas emissions from a simulated coal-burning household fire pit. *Environ. Sci. Technol.* **2008**, *42*, 2503–2508. [CrossRef]
12. Lu, S.; Hao, X.; Liu, D.; Wang, Q.; Zhang, W.; Liu, P.; Wang, Q. Mineralogical characterization of ambient fine/ultrafine particles emitted from Xuanwei C1 coal combustion. *Atmos. Res.* **2016**, *169*, 17–23. [CrossRef]
13. Gawda, A.; Majka, G.; Nowak, B.; Marcinkiewicz, J. Air pollution, oxidative stress, and exacerbation of autoimmune diseases. *Cent. Eur. J. Immunol.* **2017**, *42*, 305. [CrossRef] [PubMed]
14. Valavanidis, A.; Fiotakis, K.; Vlachogianni, T. Airborne particulate matter and human health: Toxicological assessment and importance of size and composition of particles for oxidative damage and carcinogenic mechanisms. *J. Environ. Sci. Health—Part C Environ. Carcinog. Ecotoxicol. Rev.* **2008**, *26*, 339–362. [CrossRef] [PubMed]
15. Wang, X.; Zhang, W.; Chen, H.; Liao, N.; Wang, Z.; Zhang, X.; Hai, C. High selenium impairs hepatic insulin sensitivity through opposite regulation of ROS. *Toxicol. Lett.* **2014**, *224*, 16–23. [CrossRef] [PubMed]
16. Pöschl, U.; Shiraiwa, M. Multiphase chemistry at the atmosphere–biosphere interface influencing climate and public health in the anthropocene. *Chem. Rev.* **2015**, *115*, 4440–4475. [CrossRef]
17. Arangio, A.M.; Tong, H.; Socorro, J.; Pöschl, U.; Shiraiwa, M. Quantification of environmentally persistent free radicals and reactive oxygen species in atmospheric aerosol particles. *Atmos. Chem. Phys.* **2016**, *16*, 13105–13119. [CrossRef]
18. Li, N.; Xia, T.; Nel, A.E. The role of oxidative stress in ambient particulate matter-induced lung diseases and its implications in the toxicity of engineered nanoparticles. *Free Radic. Biol. Med.* **2008**, *44*, 1689–1699. [CrossRef] [PubMed]
19. Xu, Y.; Qin, L.; Liu, G.; Zheng, M.; Li, D.; Yang, L. Assessment of personal exposure to environmentally persistent free radicals in airborne particulate matter. *J. Hazard. Mater.* **2021**, *409*, 125014. [CrossRef] [PubMed]
20. Chen, Q.; Sun, H.; Wang, J.; Shan, M.; Yang, X.; Deng, M.; Zhang, L. Long-life type—The dominant fraction of EPFRs in combustion sources and ambient fine particles in Xi'an. *Atmos. Environ.* **2019**, *219*, 117059. [CrossRef]
21. Wang, C.; Huang, Y.; Zhang, Z.; Cai, Z. Levels, spatial distribution, and source identification of airborne environmentally persistent free radicals from tree leaves. *Environ. Pollut.* **2020**, *257*, 113353. [CrossRef]
22. Qian, R.; Zhang, S.; Peng, C.; Zhang, L.; Yang, F.; Tian, M.; Chen, Y. Characteristics and potential exposure risks of environmentally persistent free radicals in PM2.5 in the three gorges reservoir area, Southwestern China. *Chemosphere* **2020**, *252*, 126425. [CrossRef] [PubMed]
23. Dellinger, B.; Lomnicki, S.; Khachatryan, L.; Maskos, Z.; Hall, R.W.; Adounkpe, J.; Truong, H. Formation and stabilization of persistent free radicals. *Proc. Combust. Inst.* **2007**, *31*, 521–528. [CrossRef] [PubMed]
24. Balakrishna, S.; Saravia, J.; Thevenot, P.; Ahlert, T.; Lominiki, S.; Dellinger, B.; Cormier, S.A. Environmentally persistent free radicals induce airway hyperresponsiveness in neonatal rat lungs. *Part. Fibre Toxicol.* **2011**, *8*, 1–13. [CrossRef] [PubMed]
25. Kelley, M.A.; Hebert, V.Y.; Thibeaux, T.M.; Orchard, M.A.; Hasan, F.; Cormier, S.A.; Dugas, T.R. Model combustion-generated particulate matter containing persistent free radicals redox cycle to produce reactive oxygen species. *Chem. Res. Toxicol.* **2013**, *26*, 1862–1871. [CrossRef]
26. Guo, X.; Zhang, N.; Hu, X.; Huang, Y.; Ding, Z.; Chen, Y.; Lian, H.Z. Characteristics and potential inhalation exposure risks of PM2.5–bound environmental persistent free radicals in Nanjing, a mega–city in China. *Atmos. Environ.* **2020**, *224*, 117355. [CrossRef]
27. Gehling, W.; Khachatryan, L.; Dellinger, B. Hydroxyl radical generation from environmentally persistent free radicals (EPFRs) in PM2.5. *Environ. Sci. Technol.* **2014**, *48*, 4266–4272. [CrossRef]
28. Xiao, K.; Wang, Q.; Lin, Y.; Wang, W.; Lu, S.; Yonemochi, S. Approval Research for Carcinogen Humic-Like Substances (HULIS) Emitted from Residential Coal Combustion in High Lung Cancer Incidence Areas of China. *Processes* **2021**, *9*, 1254. [CrossRef]
29. Lu, S.; Tan, Z.; Liu, P.; Zhao, H.; Liu, D.; Yu, S.; Wang, Q. Single particle aerosol mass spectrometry of coal combustion particles associated with high lung cancer rates in Xuanwei and Fuyuan, China. *Chemosphere* **2017**, *186*, 278–286. [CrossRef]
30. Lubick, N. Persistent free radicals: Discovery and mechanisms for health impacts. *Environ. Sci. Technol.* **2008**, *42*, 8178. [CrossRef]
31. Gehling, W.; Dellinger, B. Environmentally persistent free radicals and their lifetimes in PM2.5. *Environ. Sci. Technol.* **2013**, *47*, 8172–8178. [CrossRef]

32. Wang, Y.; Li, S.; Wang, M.; Sun, H.; Mu, Z.; Zhang, L.; Chen, Q. Source apportionment of environmentally persistent free radicals (EPFRs) in PM2.5 over Xi'an, China. *Sci. Total Environ.* **2019**, *689*, 193–202. [CrossRef] [PubMed]
33. Zhao, J.; Shi, L.; Duan, W.; Li, H.; Yi, P.; Tao, W.; Xing, B. Emission factors of environmentally persistent free radicals in PM2.5 from rural residential solid fuels combusted in a traditional stove. *Sci. Total Environ.* **2021**, *773*, 145151. [CrossRef]
34. Tan, Z.; Lu, S.; Zhao, H.; Kai, X.; Jiaxian, P.; Win, M.S.; Wang, Q. Magnetic, geochemical characterization and health risk assessment of road dust in Xuanwei and Fuyuan, China. *Environ. Geochem. Health* **2018**, *40*, 1541–1555. [CrossRef] [PubMed]
35. Tian, X.; Xiao, L.; Shen, Y.; Luo, L.; Zhang, G.; Zhang, Q.; Tian, Y. A combination of super-resolution fluorescence and magnetic resonance imaging using a Mn (ii) compound. *Inorg. Chem. Front.* **2019**, *6*, 2914–2920. [CrossRef]
36. Qiu, P.; Huang, C.; Dong, G.; Chen, F.; Zhao, F.; Yu, Y.; Wang, Y. Plasmonic Gold Nanocrystals Stimulated Efficiently Photocatalytic Nitrogen Fixation over Mo Doped W18O49 nanowires. *J. Mater. Chem.* **2021**, *9*, 25. [CrossRef]
37. Runberg, H.L.; Mitchell, D.G.; Eaton, S.S.; Eaton, G.R.; Majestic, B.J. Stability of environmentally persistent free radicals (EPFR) in atmospheric particulate matter and combustion particles. *Atmos. Environ.* **2020**, *240*, 117809. [CrossRef]
38. Chen, Q.; Sun, H.; Mu, Z.; Wang, Y.; Li, Y.; Zhang, L.; Zhang, Z. Characteristics of environmentally persistent free radicals in PM2.5: Concentrations, species and sources in Xi'an, Northwestern China. *Environ. Pollut.* **2019**, *247*, 18–26. [CrossRef]
39. Chen, Q.; Sun, H.; Song, W.; Cao, F.; Tian, C.; Zhang, Y.L. Size-resolved exposure risk of persistent free radicals (PFRs) in atmospheric aerosols and their potential sources. *Atmos. Chem. Phys.* **2020**, *20*, 14407–14417. [CrossRef]
40. Xu, Y.; Yang, L.; Wang, X.; Zheng, M.; Li, C.; Zhang, A.; Liu, G. Risk evaluation of environmentally persistent free radicals in airborne particulate matter and influence of atmospheric factors. *Ecotoxicol. Environ. Saf.* **2020**, *196*, 110571. [CrossRef]
41. Grevatt, P.C. Toxicological Review of Trivalent Chromium. 1998. Available online: http://www.epa.gov/IRIS/toxreviews/0028-tr.Pdf (accessed on 8 October 2021).
42. Chen, Q.; Wang, M.; Sun, H.; Wang, X.; Wang, Y.; Li, Y.; Mu, Z. Enhanced health risks from exposure to environmentally persistent free radicals and the oxidative stress of PM2.5 from Asian dust storms in Erenhot, Zhangbei and Jinan, China. *Environ. Int.* **2018**, *121*, 260–268. [CrossRef]
43. Tian, L.; Koshland, C.P.; Yano, J.; Yachandra, V.K.; Yu, I.T.; Lee, S.C.; Lucas, D. Carbon-centered free radicals in particulate matter emissions from wood and coal combustion. *Energy Fuels* **2009**, *23*, 2523–2526. [CrossRef] [PubMed]
44. Shaltout, A.A.; Boman, J.; Shehadeh, Z.F.; Dhaif-Allah, R.; Hemeda, O.M.; Morsy, M.M. Spectroscopic investigation of PM2.5 collected at industrial, residential and traffic sites in Taif, Saudi Arabia. *J. Aerosol Sci.* **2015**, *79*, 97–108. [CrossRef]
45. Wang, P.; Pan, B.; Li, H.; Huang, Y.; Dong, X.; Ai, F.; Xing, B. The overlooked occurrence of environmentally persistent free radicals in an area with low-rank coal burning, Xuanwei, China. *Environ. Sci. Technol.* **2018**, *52*, 1054–1061. [CrossRef] [PubMed]
46. Yang, L.; Liu, G.; Zheng, M.; Jin, R.; Zhu, Q.; Zhao, Y.; Xu, Y. Highly elevated levels and particle-size distributions of environmentally persistent free radicals in haze-associated atmosphere. *Environ. Sci. Technol.* **2017**, *51*, 7936–7944. [CrossRef] [PubMed]
47. Valavanidis, A.; Fiotakis, K.; Vlahogianni, T.; Papadimitriou, V.; Pantikaki, V. Determination of selective quinones and quinoid radicals in airborne particulate matter and vehicular exhaust particles. *Environ. Chem.* **2006**, *3*, 118–123. [CrossRef]
48. Dellinger, B.; Pryor, W.A.; Cueto, R.; Squadrito, G.L.; Hegde, V.; Deutsch, W.A. Role of free radicals in the toxicity of airborne fine particulate matter. *Chem. Res. Toxicol.* **2001**, *14*, 1371–1377. [CrossRef]
49. Ruan, X.; Sun, Y.; Du, W.; Tang, Y.; Liu, Q.; Zhang, Z.; Tsang, D.C. Formation, characteristics, and applications of environmentally persistent free radicals in biochars: A review. *Bioresour. Technol.* **2019**, *281*, 457–468. [CrossRef]
50. Huang, Y.; Guo, X.; Ding, Z.; Chen, Y.; Hu, X. Environmentally persistent free radicals in biochar derived from Laminaria japonica grown in different habitats. *J. Anal. Appl. Pyrolysis* **2020**, *151*, 104941. [CrossRef]
51. Feld-Cook, E.E.; Bovenkamp-Langlois, L.; Lomnicki, S.M. Effect of particulate matter mineral composition on environmentally persistent free radical (EPFR) formation. *Environ. Sci. Technol.* **2017**, *51*, 10396–10402. [CrossRef]
52. Chen, Q.; Sun, H.; Wang, M.; Mu, Z.; Wang, Y.; Li, Y.; Zhang, Z. Dominant fraction of EPFRs from nonsolvent-extractable organic matter in fine particulates over Xi'an, China. *Environ. Sci. Technol.* **2018**, *52*, 9646–9655. [CrossRef]
53. Liu, J.; Jiang, X.; Shen, J.; Zhang, H. Influences of particle size, ultraviolet irradiation and pyrolysis temperature on stable free radicals in coal. *Powder Technol.* **2015**, *272*, 64–74. [CrossRef]
54. Lyu, Y.; Guo, H.; Cheng, T.; Li, X. Particle size distributions of oxidative potential of lung-deposited particles: Assessing contributions from quinones and water-soluble metals. *Environ. Sci. Technol.* **2018**, *52*, 6592–6600. [CrossRef] [PubMed]
55. McFerrin, C.A.; Hall, R.W.; Dellinger, B. Ab initio study of the formation and degradation reactions of semiquinone and phenoxyl radicals. *J. Mol. Struct. THEOCHEM* **2008**, *848*, 16–23. [CrossRef]
56. Church, D.F.; Pryor, W.A. Free-radical chemistry of cigarette smoke and its toxicological implications. *Environ. Health Perspect.* **1985**, *64*, 111–126. [CrossRef] [PubMed]
57. Dugas, T.R.; Lomnicki, S.; Cormier, S.A.; Dellinger, B.; Reams, M. Addressing emerging risks: Scientific and regulatory challenges associated with environmentally persistent free radicals. *Int. J. Environ. Res. Public Health* **2016**, *13*, 573. [CrossRef]